Acta Crystallographica Section A
Foundations of Crystallography
ISSN 0108-7673

Received 20 December 2010
Accepted 25 January 2011

Grazing-incidence small-angle X-ray scattering from a random rough surface: a self-consistent wavefunction approximation

Feliks Chukhovskii

X-ray Diagnostics Methods, Institute of Crystallography RAN, Leninsky Prospect 59, 11933 Moscow, Russian Federation. Correspondence e-mail: f_chukhov@yahoo.ca

An attempt is made to go beyond the distorted-wave Born approximation addressed to the grazing-incidence small-angle X-ray (GISAX) scattering from a random rough surface. The integral wave equation adjusted with the Green function formalism is applied. To find out an asymptotic solution of the non-averaged integral wave equation in terms of the Green function formalism, the theoretical approach based on a *self-consistent* approximation for the X-ray wavefunction is elaborated. Such an asymptotic solution allows one to describe the reflected X-ray wavefield everywhere in the scattering (θ, φ) angular range, in particular below the critical angle θ_{cr} for total external reflection (θ is the grazing scattering angle with the surface, φ is the azimuth scattering angle; θ_0 is the grazing incidence angle). Analytical expressions for the reflected GISAX specular and diffuse scattering waves are obtained using the statistical model of a random Gaussian surface in terms of the r.m.s. roughness and two-point *cumulant* correlation function. For specular scattering the conventional Fresnel expression multiplied by the Debye–Waller factor is obtained. For the reflected GISAX diffuse scattering the intensity of the $R_{dif}(\theta, \varphi)$ scan is written in terms of the statistical scattering factor $\tilde{\eta}(\theta, \theta_0)$ and Fourier transform of the two-point cumulant correlation function. To be specific for isotropic solid surfaces, the statistical scattering factor $\tilde{\eta}(\theta, \theta_0)$ and Fourier transform of the two-point cumulant correlation function parametrically depend on the root-mean-square roughness σ [$\tilde{\eta}(\theta, \theta_0) = 0$ for $\sigma = 0$] and cumulant correlation length ℓ, respectively. The reflected $R_{dif}(\theta, \varphi)$ scans are numerically simulated for the typical-valued $\{\theta_0, \sigma, \ell\}$ parameters array.

1. Introduction

As is well known, the X-ray scattering technique is a powerful tool for the non-destructive characterization of solid media, thin layers and multilayered structures ranging from a few nanometres up to some micrometres (see, *e.g.*, Levine *et al.*, 1989; Pietsch *et al.*, 2004; Schmidbauer *et al.*, 2008; Gilles *et al.*, 2009; Zozulya *et al.*, 2008 and references therein). This so-called mesoscopic scale range is of physical interest and notably important for investigating the self-organized formation of semiconductor nanostructures. X-ray scattering techniques have proved to be very effective for non-destructive characterization of semiconductor quantum dots and wires (Schmidbauer *et al.*, 2008). Recently, the electron density of epitaxic SiGe nano-islands was determined using coherent scattering in grazing-incidence small-angle X-ray (GISAX) scattering (Zozulya *et al.*, 2008).

To date, many experimental and theoretical works have been reported with the GISAX scattering from rough surfaces and/or interfaces. Most of them have been concerned with the specularly reflected GISAX scattering that has been mainly interpreted in terms of the Fresnel reflection and transmission coefficients multiplied by the corresponding Debye–Waller factors. The latter are exponential factors and quadratically depend on the root-mean-square (r.m.s.) roughness σ of a random rough interface (Nevot & Croce, 1980; de Boer, 1994, 1995; Lazzari, 2002; Chukhovskii, 2009; Chukhovskii & Polyakov, 2010).

It is interesting to notice that an endeavour to go beyond the Debye–Waller approximation for the specular reflection and transmission coefficients is made in Chukhovskii & Polyakov (2010), taking into account the X-ray multiple scattering effects.

On the other hand, the reflected GISAX diffuse scattering intensity, $R_{dif}(\theta, \varphi; \theta_0)$ scan (θ is the grazing scattering angle with the surface, φ is the azimuth scattering angle; θ_0 is the grazing incidence angle), which can be recorded with the necessary resolution in all the two (three) dimensions in angular space $\{\theta, \varphi; \theta_0\}$, is notably informative (Schmidbauer *et al.*, 2008). Noteworthy is the fact that in order to describe the

reflected GISAX diffuse scattering from statistically rough surfaces, particularly peaks in $R_{\rm dif}(\theta, \varphi; \theta_0)$ scans when the incident wavevector $\mathbf{k}_0$ or scattered wavevector $\mathbf{k}$ makes an angle with the surface ($z = 0$) close to the critical angle $\theta_{\rm cr}$ for total external reflection ('Yoneda's scattering'; Yoneda, 1963), the first-order Born approximation is invalid and the distorted-wave Born approximation (DWBA) is required (Sinha *et al.*, 1988).

Quite some time ago, in the scope of the first-order perturbation theory, slightly diverse theoretical approaches aiming to solve the stationary wave equation describing the X-ray wavefield propagation within two media separated by a random rough interface were proposed (Petrashen' *et al.*, 1983; Vinogradov *et al.*, 1985). To be specific, in Vinogradov *et al.* (1985) using the conventional first-order perturbation theory in the framework of the Green function formalism the solution of the integral wave equation was obtained and the reflected $R_{\rm dif}(\theta, \varphi)$ scans have been calculated and analysed [hereafter the argument θ_0 in $R_{\rm dif}(\theta, \varphi; \theta_0)$ scan is assumed to be fixed and omitted for simplicity].

In general, the Green function formalism is a very powerful tool for the theoretical investigation of the reflected GISAX scattering. At the same time, clearly, the first-order perturbation theory has some validity provided that the parameter $\max(k_{0z}, k_z)\sigma$ is rather small. In turn, it does not yield correct quantitative results, particularly for relatively large angles $\{\theta, \theta_0\}$ of X-ray scattering, when the above-mentioned condition does not hold. While there may be similarities to the first-order perturbation theory, there remain major quantitative differences, at least.

For reference, the X-ray wavelength λ is of the order of 0.1 nm, the complex electric susceptibility $\chi \equiv {\rm Re}\chi + i{\rm Im}\chi$, ${\rm Re}\chi < 0$ and ${\rm Im}\chi > 0$. In the case under consideration the X-ray wavelength λ is of the order of 0.1 nm, ${\rm Re}\chi \simeq -10^{-5}$ and ${\rm Im}\chi \simeq 0.05|{\rm Re}\chi|$ are assumed.

A challenge in the reflected GISAX scattering is the issue of determining the medium density associated with the critical angle for total external reflection, $\theta_{\rm cr} = (-{\rm Re}\chi)^{1/2}$, and the r.m.s. interface roughness σ from the experimental $R_{\rm dif}(\theta, \varphi)$ scan and/or alternatively specular reflectivity data. In fact, most of the experimental and theoretical studies of the GISAX scattering from statistically random surfaces and/or interfaces have been carried out over the wide angular range of X-ray scattering, $\max\{\theta, \theta_0\} > \theta_{\rm cr}$, and the r.m.s. roughnesses σ that are of the order of a few nanometres (*e.g.* Petrashen' *et al.*, 1983; Vinogradov *et al.*, 1985; Sinha *et al.*, 1988; Pietsch *et al.*, 2004; Bridou *et al.*, 2006; Chukhovskii, 2009). Clearly, the conventional first-order perturbation theory is invalid when the reflected X-ray wavefield amplitude becomes of the order of unity (*e.g.* below the critical angle $\theta_{\rm cr}$ for total external reflection). The DWBA method consists of evaluating the first-order scattering matrix element between the Fresnel wavefunction eigenstates (Sinha *et al.*, 1988). At the same time, how to choose and evaluate the perturbation matrix element is rather complicated and not evident from the mathematical and physical viewpoint. Despite these limitations, with due care the DWBA method was needed to describe the reflected GISAX scattering when the r.m.s. roughness σ is not relatively small, at least.

The Green function formalism may be applied for solving the integral wave equation in an attempt to go beyond the DWBA method. It is hoped that the Green function formalism is favourable if it concerns a quantitative analysis of the reflected GISAX diffuse scattering $R_{\rm dif}(\theta, \varphi)$ scans and one aims to retrieve the physical surface parameters of interest neither supposing a relative smallness of the r.m.s. roughness σ nor using the first-order Born approximation.

In this paper, the concept of the Green function formalism is pushed one step further and applied to describing the GISAX scattering from a statistically rough interface of two homogeneous media. A prerequisite for solving the integral wave equation is to develop a new approach based on an appropriate *self-consistent* approximation for the wavefunction and achieve results beyond the DWBA method.

In §2, as a compound of the Green function formalism, the integral wave equation describing the GISAX wavefield propagation within two media separated from each other by a random rough interface is briefly derived (*cf.* Vinogradov *et al.*, 1985). As a kernel function, such an integral equation contains the Green (point-source) function of a twofold medium with a flat interface. From the mathematical viewpoint the appropriate Green function is a bilinear combination of the two linearly independent wavefunction *eigenstates*. Physically, both these wavefunctions are the conventional Fresnel solutions for the GISAX scattering issue in terms of the plane waves propagating within a twofold flat-interface medium in the *direct* and *mirror-reversed* scattering geometry.

In §3, using the wavefunction approximation in a self-consistent sense (*cf.* Chukhovskii & Polyakov, 2010), an asymptotic non-averaged solution of the integral wave equation for the reflected GISAX scattering issue is carried out. Herein, the key idea is to approximate the wavefunction under integration in the integral wave equation by the pseudo-plane wavefunction that includes some phase factors provided its continuity at the actual rough interface.

In §4, the statistical model of a random rough surface in terms of the two-point *cumulant* correlation function $g_2(|\mathbf{x}_1 - \mathbf{x}_2|/\ell)$ is applied. Such a correlation function $g_2(|\mathbf{x}_1 - \mathbf{x}_2|/\ell)$ was first introduced by Kato (1980) for describing the X-ray diffraction in statistically distorted crystals. Generally, the function $g_2(|\mathbf{x}_1 - \mathbf{x}_2|/\ell) = 1$ for $\mathbf{x}_1 = \mathbf{x}_2$ and $g_2(|\mathbf{x}_1 - \mathbf{x}_2|/\ell) \rightarrow 0$ for $|\mathbf{x}_1 - \mathbf{x}_2|/\ell \rightarrow \infty$, the vector $\mathbf{x} \equiv \mathbf{x}_1 - \mathbf{x}_2$ is directed along the averaged flat surface ($z = 0$), ℓ is the cumulant correlation length.

Then, in the scope of the Gaussian statistics, the analytical expressions for the statistical scattering factor $\tilde{\eta}(\theta, \theta_0)$ and reflected $R(\theta, \varphi)$ scan for the X-ray radiation of specular and diffuse wavefield components are derived. Unlike the Nevot–Croce factor in the DWBA for the reflected specular wave (Sinha *et al.*, 1988), there now occurs the conventional Debye–Waller factor.

In §5, the numerically calculated results related to the normalized statistical scattering factors $\eta(\theta, \theta_0)$ and reflected diffuse scattering $R_{\rm dif}(\theta, \varphi)$ scans are presented and analysed

depending on a dimensionless parameters array $\{k\sigma, k\ell, \theta_0/\theta_{cr}\}$ of interest.

2. Green function formalism

Let the incident unit plane wave $E_{inc}(\mathbf{r}) = \exp(i\mathbf{k}_0\mathbf{r})$ impinge on a rough interface separating vacuum and medium. The X-ray wavefield component polarized parallel to the averaged flat surface $z = 0$ (TE polarization) is assumed to be under consideration; $\mathbf{k}_0 = (\mathbf{q}_0, k_{0z})$ is the incident wavevector, $\mathbf{q}_0$ is the lateral wavevector component, $k_{0z} = (k^2 - \mathbf{q}_0{}^2)^{1/2}$ is the internal-normal wavevector component, $k = |\mathbf{k}_0|$ is the wavenumber in a vacuum.

In the case of TE-polarized X-ray radiation the stationary wave equation holds everywhere (recall that in the case of the X-ray radiation polarized perpendicular to a plane formed by the TE polarization vector and the incident wavevector, TM polarization, for grazing incidence there are the same results as for TE polarization; see, *e.g.*, Sinha *et al.*, 1988),

$$\{\nabla^2 + k^2[1 + \chi\Theta(z)]\}E(\mathbf{r}) = -k^2\Delta\chi(\mathbf{r})E(\mathbf{r}), \qquad (1)$$

where $E(\mathbf{r})$ is the wavefunction for the TE-polarized electric wavefield and

$$\Delta\chi(\mathbf{r}) = \chi\{\Theta[z - h(\mathbf{x})] - \Theta(z)\}, \qquad (2)$$

$h(\mathbf{x})$ is the height of an actual rough surface at the point $\mathbf{x}$ (assumed to be single valued); $\Theta(z)$ is the unit step function: $\Theta(z) = 1$ for $z > 0$ and $\Theta(z) = 0$ for $z < 0$.

According to the Green function formalism the wave equation (1) can be written in the integral form as (*cf.* Vinogradov *et al.*, 1985)

$$E(\mathbf{r}) = E_0(\mathbf{r}) - k^2 \int \mathrm{d}^3\mathbf{r}'\, \mathbf{G}(\mathbf{r}, \mathbf{r}')\Delta\chi(\mathbf{r}')E(\mathbf{r}'). \qquad (3)$$

Herein, the Green (point-source) function $\mathrm{G}(\mathbf{r}, \mathbf{r}')$ is given by

$$\mathbf{G}(\mathbf{r}, \mathbf{r}') = -i(4\pi)^{-2} \int \mathrm{d}^2\mathbf{q}\big[k_z^{-1}(q) + \kappa_z^{-1}(q)\big] \times \exp[i\mathbf{q}(\mathbf{x} - \mathbf{x}')]\begin{cases} y_2(z, q)y_1(z', q), & z \le z' \\ y_1(z, q)y_2(z', q), & z \ge z' \end{cases} \qquad (4)$$

everywhere in a twofold medium with the step-like electric susceptibility $\chi(\mathbf{r}) = \chi\Theta(z)$.

The functions $y_1(z, q)$ and $y_2(z, q)$ are the two linearly independent solutions of the wave equation

$$(\mathrm{d}^2y/\mathrm{d}z^2) + \{k^2[1 + \chi\Theta(z)] - q^2\}y = 0 \qquad (5)$$

over the variable z.

These functions can be chosen in the form of the conventional Fresnel solutions

$$y_1(z, q) = \begin{cases} \exp[ik_z(q)z] + R_1(q)\exp[-ik_z(q)z] & \text{for} \quad z \le 0 \\ T_1(q)\exp[i\kappa_z(q)z] & \text{for} \quad z \ge 0, \end{cases}$$
$$y_2(z, q) = \begin{cases} T_2(q)\exp[-ik_z(q)z] & \text{for} \quad z \le 0 \\ \exp[-i\kappa_z(q)z] + R_2(q)\exp[i\kappa_z(q)z] & \text{for} \quad z \ge 0 \end{cases} \qquad (6)$$

in the direct and mirror-reversed scattering geometry.

In the case of a twofold medium with the averaged flat interface $z = 0$, the Fresnel reflection coefficients, $R_1(q)$ and $R_2(q)$, and transmission, $T_1(q)$ and $T_2(q)$, coefficients take the form

$$R_1(q) = \frac{k_z(q) - \kappa_z(q)}{k_z(q) + \kappa_z(q)} \quad \text{and} \quad R_2(q) = \frac{\kappa_z(q) - k_z(q)}{k_z(q) + \kappa_z(q)},$$
$$T_1(q) = \frac{2k_z(q)}{k_z(q) + \kappa_z(q)} \quad \text{and} \quad T_2(q) = \frac{2\kappa_z(q)}{k_z(q) + \kappa_z(q)}, \qquad (7)$$

where the wavevector components $k_z(q)$ and $\kappa_z(q)$ with the same lateral component $\mathbf{q}$ in a vacuum and medium are introduced as follows [the vector $\mathbf{q}$ is parallel to the plane $z = 0$, $\kappa^2 = k^2(1 + \chi)$]

$$k_z(q) = (k^2 - q^2)^{1/2},$$
$$\kappa_z(q) = (\kappa^2 - q^2)^{1/2}. \qquad (8)$$

It is easily seen that owing to the *pure* incoming plane wave $E_{inc}(\mathbf{r}) = \exp(i\mathbf{k}_0\mathbf{r})$, the free term $E_0(\mathbf{r})$ on the right-hand side of the integral wave equation (3) should take the form

$$E_0(\mathbf{r}) = \exp(i\mathbf{q}_0\mathbf{x})y_1(z, q_0). \qquad (9)$$

Noteworthy is the fact that, as seen from the integral wave equation (3), beyond the integration procedure over the variables $(\mathbf{q}, \mathbf{x})$, the integration range over the variable z is defined by $\{\Theta[z - h(\mathbf{x})] - \Theta(z)\}$ and determines the asymptotic behaviour of the wavefunction $E(\mathbf{x}, z)|_{z \to -\infty}$, which physically describes the reflected GISAX scattering.

It is easily shown that implementing the perturbation theory over solution of the integral wave equation (3) with substituting expression (9) as the initial wavefunction approximation into its right-hand side is effective, provided the small-valued parameter $\max[k_{0z}(q_0), k_z(q)]\sigma$ (Vinogradov *et al.*, 1985). If the aforementioned parameter is of the order of unity or more, as is well known, the first-order perturbation theory approximation does not hold. While there may be similarities to the first-order perturbation theory, there may remain some differences with regard to qualitative features of the GISAX scattering from a random rough surface, in the best case.

3. Self-consistent approximation

To overcome the problem, we will attempt to modify the basic wavefunction approximation for solving the non-averaged integral wave equation (3). A relevant procedure utilizes the first-order perturbation theory as well but the wavefunction on the right of equation (3) can be relatively well approximated in a self-consistent sense as

$$E[\mathbf{x}, z; h(\mathbf{x})] \cong \exp(i\mathbf{q}_0\mathbf{x}) \times \begin{cases} \exp[ik_z(q_0)z] + R_1(q_0)\exp\{-ik_z(q_0)[z - 2h(\mathbf{x})]\} \text{ for } z \le h(\mathbf{x}) \\ T_1(q_0)\exp\{i[k_z(q_0) - \kappa_z(q_0)]h(\mathbf{x}) + i\kappa_z(q_0)z\} \text{ for } z \ge h(\mathbf{x}). \end{cases} \qquad (10)$$

Unlike the free-term wavefunction (9), expression (10) is chosen as the pseudo-plane wavefunction with some exponential factors that provide the wavefunction continuity at an

actual rough surface $z = h(\mathbf{x})$ (*cf.* Chukhovskii & Polyakov, 2010).

Staying in the framework of the self-consistent wavefunction approximation [equation (10)] and substituting it into the right-hand side of the integral wave equation (3), after the straightforward routine calculations for the Fourier transform of the asymptotic wavefunction $E(\mathbf{q}, z)$ one obtains ($z \to -\infty$)

$$E(\mathbf{q}, z) = (2\pi)^2\delta_2(\mathbf{q}-\mathbf{q}_0)[\exp(ik_z z) + R_1(q_0)\exp(-ik_z z)] + f(\mathbf{q}, \mathbf{q}_0)\exp[-ik_z(q)z]. \quad (11)$$

Above, the *scattering amplitude* $f(\mathbf{q}, \mathbf{q}_0)$ is properly determined as the Fourier transform

$$f(\mathbf{q}, \mathbf{q}_0) = -\frac{\chi k^2}{2k_z(\mathbf{q})}\int \mathrm{d}^2\mathbf{x}\exp[i\mathbf{x}(\mathbf{q}_0-\mathbf{q})]Z[q, q_0, h(\mathbf{x})], \quad (12)$$

where

$$\begin{aligned} &Z[q, q_0, h(\mathbf{x})] \\ &= T_1(q)\left(\frac{\exp\{i[k_z(q_0)+\kappa_z(q)]h(\mathbf{x})\}-1}{k_z(q_0)+\kappa_z(q)}\right. \\ &\quad \left. + R_1(q_0)\exp[2ik_z(q_0)h(\mathbf{x})]\frac{\exp\{i[-k_z(q_0)+\kappa_z(q)]h(\mathbf{x})\}-1}{-k_z(q_0)+\kappa_z(q)}\right) \\ &\quad \text{for } h(\mathbf{x}) \geq 0, \\ &= T_1(q_0)\exp\{i[k_z(q_0)-\kappa_z(q_0)]h(\mathbf{x})\} \\ &\quad \times\left(\frac{\exp\{i[k_z(q)+\kappa_z(q_0)h(\mathbf{x})]\}-1}{k_z(q)+\kappa_z(q_0)}\right. \\ &\quad \left. + R_1(q)\frac{\exp\{i[-k_z(q)+\kappa_z(q_0)h(\mathbf{x})]\}-1}{-k_z(q)+\kappa_z(q_0)}\right) \\ &\quad \text{for } h(\mathbf{x}) \leq 0 \end{aligned} \quad (13)$$

is the non-averaged complex *scattering length* along the z axis, for evaluating that the Green function presentation [equation (4)] as well as explicit expressions (6)–(7) were directly utilized.

Except for the term of the incident plane wave such that $(2\pi)^2\delta_2(\mathbf{q}-\mathbf{q}_0)\exp(ik_z z)$, expressions (11)–(12) can be used to evaluate the reflected GISAX intensity distribution [$\delta_2(\mathbf{q}-\mathbf{q}_0)$ is the two-dimensional delta function]

$$\frac{\mathrm{d}R(\theta,\varphi)}{\mathrm{d}\Omega} = (2\pi)^{-2}k^2\frac{\sin^2\theta}{\sin\theta_0} \times S_2^{-1}\overline{|\,(2\pi)^2\delta_2(\mathbf{q}-\mathbf{q}_0)R_1(q_0)+f(\mathbf{q},\mathbf{q}_0)\,|^2}, \quad (14)$$

that is statistically averaged over the random rough surface.

For reference, the symbol $\overline{|\ldots|^2}$ indicates an average procedure, $\mathrm{d}\Omega = \cos\theta\,\mathrm{d}\theta\,\mathrm{d}\varphi$ is the elementary solid angle for the reflected beam, S_2 is an area of the reference surface illuminated by incident X-rays.

To fulfill an average procedure on expression (14) under consideration in the explicit form, one has to specify a statistical model of the surface and then averaging equation (14) may be carried out.

4. Averaging over a random rough surface – the two-point cumulant correlation function

As is already known (see, *e.g.*, Sinha *et al.*, 1988; Chukhovskii & Polyakov, 2010), the statistical properties of a random rough surface are defined in terms of the r.m.s. roughness $\sigma = [\overline{h(\mathbf{x})^2}]^{1/2}$ and height–height correlation function

$$K_2(|\mathbf{x}-\mathbf{s}|/\xi) = \sigma^{-2}\overline{h(\mathbf{x})h(\mathbf{s})}, \quad (15)$$

where ξ is the height–height correlation length along the isotropic surface.

For many isotropic solid surfaces such a function can be written as

$$K_2(|\mathbf{x}-\mathbf{s}|/\xi) = \exp[-(|\mathbf{x}-\mathbf{s}|/\xi)^{2(3-D_s)}] \quad (2 < D_s < 3) \quad (16)$$

where the real value D_s is the self-affine surface fractal dimension which determines the texture of the surface roughness (Mandelbrodt, 1982; Voss, 1985). For instance, values of D_s approaching 2 produce various kinds of physical surfaces like smooth hills and valleys. The height–height correlation function given by expression (16) is of physical interest, since it totally embraces properties of the so-called self-affine surfaces (Sinha *et al.*, 1988).

To clarify the statistical properties of the random rough surface and, in particular, evaluate the reflected GISAX intensity [equation (14)], we will utilize the result that if $B[h(\mathbf{x})]$ is a fluctuating quantity, then

$$\begin{aligned} &\overline{|A + \int \mathrm{d}^2\mathbf{x}\exp[i(\mathbf{q}_0-\mathbf{q})\mathbf{x}]B[h(\mathbf{x})]|^2} \\ &= |A + \overline{B[h(\mathbf{x})]}\int \mathrm{d}^2\mathbf{x}\exp[i(\mathbf{q}_0-\mathbf{q})\mathbf{x}]|^2 \\ &\quad + \left\{\overline{B[h(\mathbf{x})]B^*[h(\mathbf{x})]} - |\overline{B[h(\mathbf{x})]}|^2\right\}S_2 \\ &\quad \times \int \mathrm{d}^2\mathbf{x}\exp[i(\mathbf{q}_0-\mathbf{q})\mathbf{x}]g_2[|\mathbf{x}|/\ell] \end{aligned} \quad (17)$$

is the identity for a non-fluctuating term A.

The second term on the right relates to the reflected GISAX diffuse scattering and is proportional to the Fourier transform of the two-point cumulant correlation function $g_2(|\mathbf{x}_1-\mathbf{x}_2|/\ell)$ that was first introduced by Kato (1980) for describing the X-ray diffraction by statistically imperfect crystalline media so that $g_2(|\mathbf{x}_1-\mathbf{x}_2|/\ell) = 1$ for $\mathbf{x}_1 = \mathbf{x}_2$ and $g_2(|\mathbf{x}_1-\mathbf{x}_2|/\ell)$ tends to zero for $|\mathbf{x}_1-\mathbf{x}_2| \to \infty$, ℓ is the cumulant correlation length, $k\ell >> 1$ (*cf.* Polyakov *et al.*, 1991).

Using equations (14) and (17) for a random Gaussian surface, after straightforward evaluations one finds that the reflected intensity distribution

$$\frac{\mathrm{d}R(\theta,\varphi)}{\mathrm{d}\Omega} = R_{\mathrm{spec}}(\mathbf{q}, \mathbf{q}_0) + R_{\mathrm{dif}}(\mathbf{q}, \mathbf{q}_0) \quad (18)$$

can be properly split into a specular and a diffuse part.

The first term on the right yields the specular reflection modified by the Debye–Waller factor $f_R{}^2$ {recall that $f_R = \exp[-2k_z{}^2(q_0)\sigma^2]$},

$$R_{\mathrm{spec}}(\mathbf{q}, \mathbf{q}_0) = k^2\frac{\sin^2\theta}{\sin\theta_0}\delta_2(\mathbf{q}-\mathbf{q}_0)|R_1(q_0)|^2 f_R^2, \quad (19)$$

and the second term on the right yields the diffuse scattering and is written as

$$R_{\rm dif}(\mathbf{q},\mathbf{q}_0) = (2\pi)^{-2}|\chi|^2 \frac{\sin^2\theta}{\sin\theta_0}\frac{k^6}{4k_z^2(q)}\tilde{\eta}(q,q_0) \times \int \mathrm{d}^2\mathbf{x}\exp[i(\mathbf{q}_0-\mathbf{q})\mathbf{x}]g_2(|\mathbf{x}|/\ell). \quad (20)$$

Herein, the *statistical scattering* factor $\tilde{\eta}(q,q_0)$ is given by [*cf.* equations (12), (13), (17)]

$$\tilde{\eta}(q,q_0) = \overline{|\,Z(q,q_0,h)Z^*(q,q_0,h)\,|} - \overline{Z(q,q_0,h)\,|^2}, \quad (21)$$

where the evaluated averages $\overline{Z(q,q_0,h)Z^*(q,q_0,h)}$ and $\left|\overline{Z(q,q_0,h)}\right|^2$ take the following forms:

$$\begin{aligned}
&\overline{Z(q,q_0,h)Z^*(q,q_0,h)}\\
&= 0.5|a|^2\Big\{\exp[-0.5\sigma^2(\alpha-\alpha^*)^2]\mathrm{Erfc}[-i(\alpha-\alpha^*)\sigma/2^{1/2}]\\
&\quad - 2\mathrm{Re}[\exp(-0.5\sigma^2\alpha^2)\mathrm{Erfc}(-i\alpha\sigma/2^{1/2})] + 1\Big\}\\
&+ 0.5|b|^2\Big\{\exp[-0.5\sigma^2(\beta-\beta^*)^2]\mathrm{Erfc}[-i(\beta-\beta^*)\sigma/2^{1/2}]\\
&\quad - 2\mathrm{Re}[\exp(-0.5\sigma^2\beta^2)\mathrm{Erfc}(-i\beta\sigma/2^{1/2})] + 1\Big\}\\
&+ \mathrm{Re}\Big(ab^*\Big\{\exp[-0.5\sigma^2(\alpha-\beta^*-\gamma)^2]\mathrm{Erfc}[-i(\alpha-\beta^*-\gamma)\sigma/2^{1/2}]\\
&\quad - \exp[-0.5\sigma^2(\alpha-\gamma)^2]\mathrm{Erfc}[-i(\alpha-\gamma)\sigma/2^{1/2}]\\
&\quad - \exp[-0.5\sigma^2(\beta^*+\gamma)^2]\mathrm{Erfc}[i(\beta^*+\gamma)\sigma/2^{1/2}]\\
&\quad + \exp(-0.5\sigma^2\gamma^2)\mathrm{Erfc}(i\gamma\sigma/2^{1/2})\Big\}\Big)\\
&+ 0.5|c|^2\Big\{\exp[-0.5\sigma^2(\mu+\zeta-\zeta^*-\mu^*)^2]\mathrm{Erfc}[i(\mu+\zeta-\zeta^*-\mu^*)\sigma/2^{1/2}]\\
&\quad - \exp[-0.5\sigma^2(\mu+\zeta-\zeta^*)^2]\mathrm{Erfc}[i(\mu+\zeta-\zeta^*)\sigma/2^{1/2}]\\
&\quad - \exp[-0.5\sigma^2(\zeta-\zeta^*-\mu^*)^2]\mathrm{Erfc}[i(\zeta-\zeta^*-\mu^*)\sigma/2^{1/2}]\\
&\quad + \exp[-0.5\sigma^2(\zeta-\zeta^*)^2]\mathrm{Erfc}[i(\zeta-\zeta^*)\sigma/2^{1/2}]\Big\}\\
&+ 0.5|d|^2\Big\{\exp[-0.5\sigma^2(\nu+\zeta-\zeta^*-\nu^*)^2]\mathrm{Erfc}[i(\nu+\zeta-\zeta^*-\nu^*)\sigma/2^{1/2}]\\
&\quad - \exp[-0.5\sigma^2(\nu+\zeta-\zeta^*)^2]\mathrm{Erfc}[i(\nu+\zeta-\zeta^*)\sigma/2^{1/2}]\\
&\quad - \exp[-0.5\sigma^2(\zeta-\zeta^*-\nu^*)^2]\mathrm{Erfc}[i(\zeta-\zeta^*-\nu^*)\sigma/2^{1/2}]\\
&\quad + \exp[-0.5\sigma^2(\zeta-\zeta^*)^2]\mathrm{Erfc}[i(\zeta-\zeta^*)\sigma/2^{1/2}]\Big\}\\
&+ \mathrm{Re}\Big(cd^*\Big\{\exp[-0.5\sigma^2(\mu+\zeta-\zeta^*-\nu^*)^2]\mathrm{Erfc}[i(\mu+\zeta-\zeta^*-\nu^*)\sigma/2^{1/2}]\\
&\quad - \exp[-0.5\sigma^2(\mu+\zeta-\zeta^*)^2]\mathrm{Erfc}[i(\mu+\zeta-\zeta^*)\sigma/2^{1/2}]\\
&\quad - \exp[-0.5\sigma^2(\zeta-\zeta^*-\nu^*)^2]\mathrm{Erfc}[i(\zeta-\zeta^*-\nu^*)\sigma/2^{1/2}]\\
&\quad + \exp[-0.5\sigma^2(\zeta-\zeta^*)^2]\mathrm{Erfc}[i(\zeta-\zeta^*)\sigma/2^{1/2}]\Big\}\Big), \quad (22)
\end{aligned}$$

and

$$\begin{aligned}
&|\overline{Z(q,q_0,h)}|^2\\
&= 0.25\Big|a\Big[\exp(-0.5\sigma^2\alpha^2)\mathrm{Erfc}(-i\sigma\alpha/2^{1/2}) - 1\Big]\\
&\quad + b\Big\{\exp[-0.5\sigma^2(\beta+\gamma)^2]\mathrm{Erfc}[-i\sigma(\beta+\gamma)/2^{1/2}]\\
&\quad\quad - \exp(-0.5\sigma^2\gamma^2)\mathrm{Erfc}(-i\sigma\gamma/2^{1/2})\Big\}\\
&\quad + c\Big\{\exp[-0.5\sigma^2(\mu+\zeta)^2]\mathrm{Erfc}[i\sigma(\mu+\zeta)/2^{1/2}]\\
&\quad\quad - \exp(-0.5\sigma^2\zeta^2)\mathrm{Erfc}(i\sigma\zeta/2^{1/2})\Big\}\\
&\quad + d\Big\{\exp[-0.5\sigma^2(\nu+\zeta)^2]\mathrm{Erfc}[i\sigma(\nu+\zeta)/2^{1/2}]\\
&\quad\quad - \exp(-0.5\sigma^2\zeta^2)\mathrm{Erfc}(i\sigma\zeta/2^{1/2})\Big\}\Big|^2. \quad (23)
\end{aligned}$$

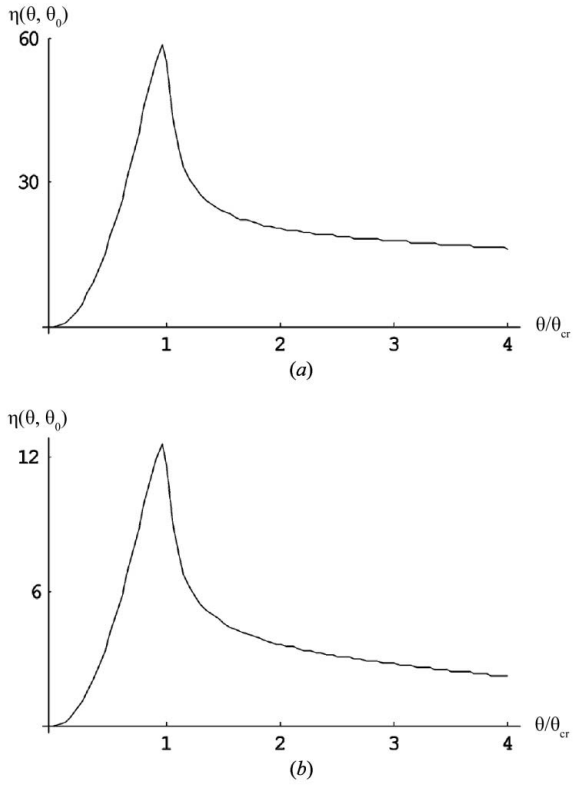

Figure 1
The normalized statistical scattering factor $\eta(\theta,\theta_0)$ *versus* the grazing scattering angle $\theta/\theta_{\rm cr}$. The critical angle $\theta_{\rm cr} = (10)^{-5/2}$. The grazing incidence angle $\theta_0/\theta_{\rm cr}$: (*a*) = 2, (*b*) = 3. The dimensionless r.m.s. roughness $k\sigma = 35$.

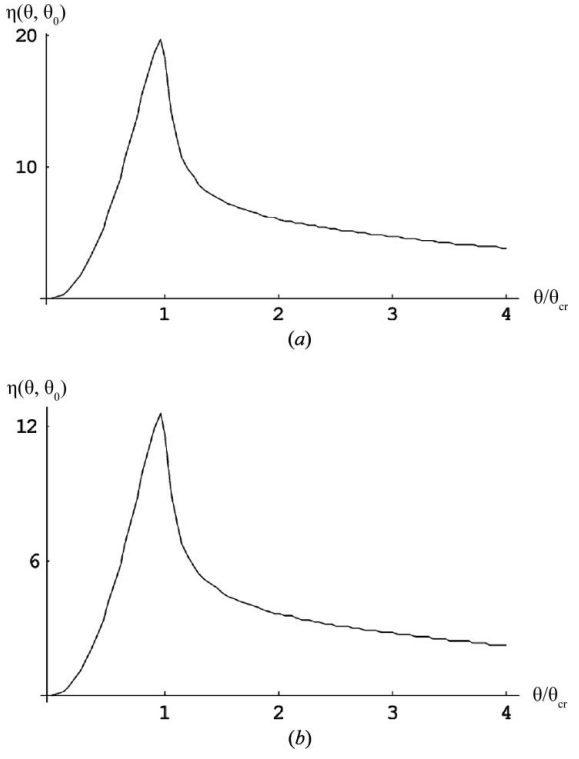

Figure 2
The normalized statistical scattering factor $\eta(\theta,\theta_0)$ *versus* the grazing scattering angle $\theta/\theta_{\rm cr}$. The critical angle $\theta_{\rm cr} = (10)^{-5/2}$. The grazing incidence angle $\theta_0/\theta_{\rm cr}$: (*a*) = 2, (*b*) = 3. The dimensionless r.m.s. roughness $k\sigma = 65$.

Above, there is the complementary error function Erfc[w] for complex w, and some combinations $\{\alpha, \beta, \gamma, \mu, \nu, \zeta\}$ of z-component wavevectors and partial *scattering lengths* $\{a, b, c, d\}$ related to diverse X-ray scattering processes are defined as

$$\alpha = k_z(q_0) + \kappa_z(q);\ \beta = -k_z(q_0) + \kappa_z(q);\ \gamma = 2k_z(q_0);$$
$$\mu = k_z(q) + \kappa_z(q_0);\ \nu = -k_z(q) + \kappa_z(q_0);\ \zeta = k_z(q_0) - \kappa_z(q_0);$$
$$a = T_1(q)/[\kappa_z(q) + k_z(q_0)],\ b = T_1(q)R_1(q_0)/[\kappa_z(q) - k_z(q_0)],$$
$$c = T_1(q_0)/[\kappa_z(q_0) + k_z(q)],\ d = T_1(q_0)R_1(q)/[\kappa_z(q_0) - k_z(q)]. \quad (24)$$

As follows from equations (23)–(24), the Gaussian-averaged complex scattering length $\overline{Z(q_0, q_0, h)}$ that concerns the GISAX specular reflection is equal to (one puts $q = q_0$ and $\alpha = \mu$, $\beta = \nu = -\zeta$, $\alpha = \beta + \gamma$; $a = c = -b = -d$ at specular)

$$\overline{Z(q_0, q_0, h)} = \left[1 - \exp(-0.5\sigma^2\gamma^2)\right]\frac{2k_z(q_0)R_1(q_0)}{\chi k^2}. \quad (25)$$

As a result, expression (19) is nothing but the specular Fresnel reflection intensity $R_{\rm spec}(\mathbf{q}, \mathbf{q}_0)$ *versus* the variable $\mathbf{q}$ along with the Debye–Waller factor ${f_{\rm R}}^2$, unlike the Nevot–Croce factor as has been previously obtained using the DWBA (Sinha *et al.*, 1988).

Before proceeding further, one needs to make the following comment. As pointed out by Sinha *et al.* (1988), the optical theorem, the basic principle of the scattering theory, is not satisfied by the first-order Born approximation or the DWBA. At present, there are no proofs that the first-order self-consistent approximation [equation (10)] for solving the basic integral wave equation (3) automatically provides the optical theorem implementation. This theoretical issue is opened for future work in the scope of the rigorous GISAX scattering approach. Such an approach does not use any perturbation theory and is based on implementation of a *cumulant average* diagram technique that allows one to transform the non-averaged wave equation (3) to the Bethe–Salpeter equation describing the GISAX diffuse scattering from statistically rough surfaces (*cf.* Polyakov *et al.*, 1991).

In-depth analysis of expressions (20)–(23) shows that the statistical scattering factor $\tilde{\eta}(q, q_0)$ reduces to $\sigma^2|T_1(q)|^2|T_1(q_0)|^2 + 0(\sigma^3)$ provided that the inequality $\sigma \times \max[|\alpha|, |\beta + \gamma|, |\gamma|, |\mu + \zeta|, |\nu + \zeta|, |\zeta|] << 1$ holds, and then expression (20) goes over to the corresponding one for the reflected GISAX diffuse scattering in the first-order Born approximation as expected (Vinogradov *et al.*, 1985). For this, when the incident wavevector $\mathbf{k}_0$ along with $q_0 = k\cos\theta_0$, or scattered wavevector $\mathbf{k}$ along with $q = k\cos\theta$, makes a grazing angle close to $\theta_{\rm cr}$ the statistical scattering factor $\tilde{\eta}(q, q_0)$ has a maximum owing to $|T_1(q)|^2$ or $|T_1(q_0)|^2$.

On the other hand, one may expect that in a general case when the aforementioned inequality fails the statistical scattering factor $\tilde{\eta}(q, q_0)$ *versus* argument q may reach a maximum at the grazing scattering angle θ close to $\theta_{\rm cr}$ [see the numerically calculated $\tilde{\eta}(q, q_0)$ in the next section]. The result is that the reflected GISAX diffuse scattering intensity $R_{\rm dif}(\mathbf{q}, \mathbf{q}_0)$ *versus* $q = k\cos\theta$ can have a peak (Yoneda, 1963) whenever θ or θ_0 is equal to $\theta_{\rm cr}$.

Going one step further, to evaluate the diffuse scattering intensity according to equation (20), we will approximate the two-point cumulant correlation function $g_2(|\mathbf{x}|/\ell)$ as

$$g_2(|\mathbf{x}|/\ell) = \exp[-|\mathbf{x}|/\ell)]. \quad (26)$$

Substituting equation (26) into the right-hand side of equation (20) and evaluating the Fourier transform of the function $g_2(|\mathbf{x}|/\ell)$ yields

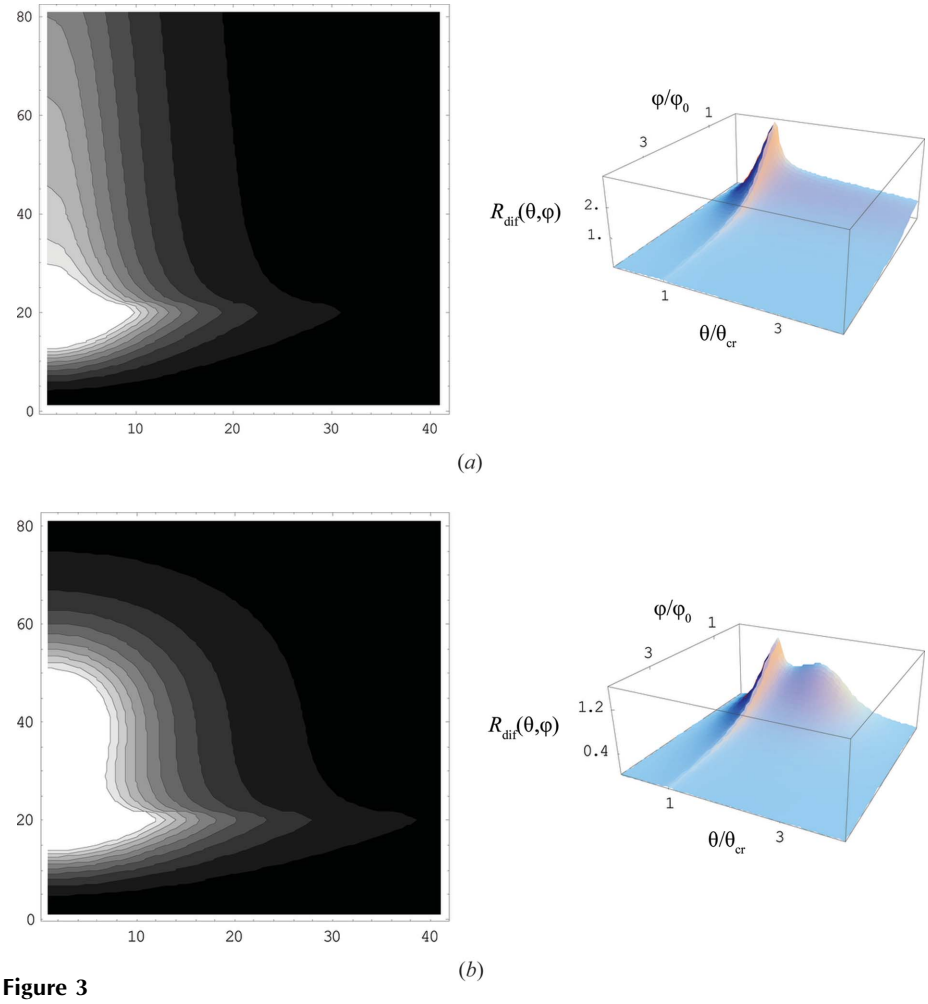

Figure 3
The numerically simulated two-dimensional contour plot and three-dimensional plot of the normalized GISAX $R_{\rm dif}(\theta, \varphi)/R_{\rm dif}(\theta_0, 0)$ scans. The grazing incidence angle $\theta_0/\theta_{\rm cr} = 2$. The dimensionless r.m.s. roughness $k\sigma = 35$. The dimensionless cumulant correlation length $k\ell$: (*a*) = 5×10^3, (*b*) = 5×10^4.

$$R_{\rm dif}(\mathbf{q},\mathbf{q}_0)=\frac{|\chi|^2k^2\tilde{\eta}(q,q_0)}{8\pi\sin\theta_0}\times\frac{k^2\ell^2}{\{1+k^2\ell^2[(\cos\theta\cos\varphi-\cos\theta_0)^2+\cos^2\theta\sin^2\varphi]\}^{3/2}}. \quad (27)$$

It is easy to show that for $k\ell\theta_0 >> 1$ the reflected GISAX diffuse scattering intensity $R_{\rm dif}(\mathbf{q},\mathbf{q}_0)$ seems to be similar to the two-dimensional delta function $\delta_2(\mathbf{q}-\mathbf{q}_0)$.

Then, one can simply obtain the upper estimate of the integrated intensity of diffuse scattering $R_{\rm dif}^{\rm (int)}(\mathbf{q}_0)$ as follows ($\sigma\neq 0$):

$$R_{\rm dif}^{\rm (int)}(\mathbf{q}_0)\Rightarrow(1-f_{\rm R})^2|R_1(q_0)|^2\eta(q_0,q_0), \quad (28)$$

where

$$\eta(q,q_0)=\left[\frac{|\,\overline{Z(q,q_0,h)Z^*(q,q_0,h)}\,|}{|\,\overline{Z(q,q_0,h)}\,|^2}-1\right] \quad (29)$$

is the normalized statistical scattering factor [*cf.* equations (21), (25)] and assuming $q=q_0$ in equation (29).

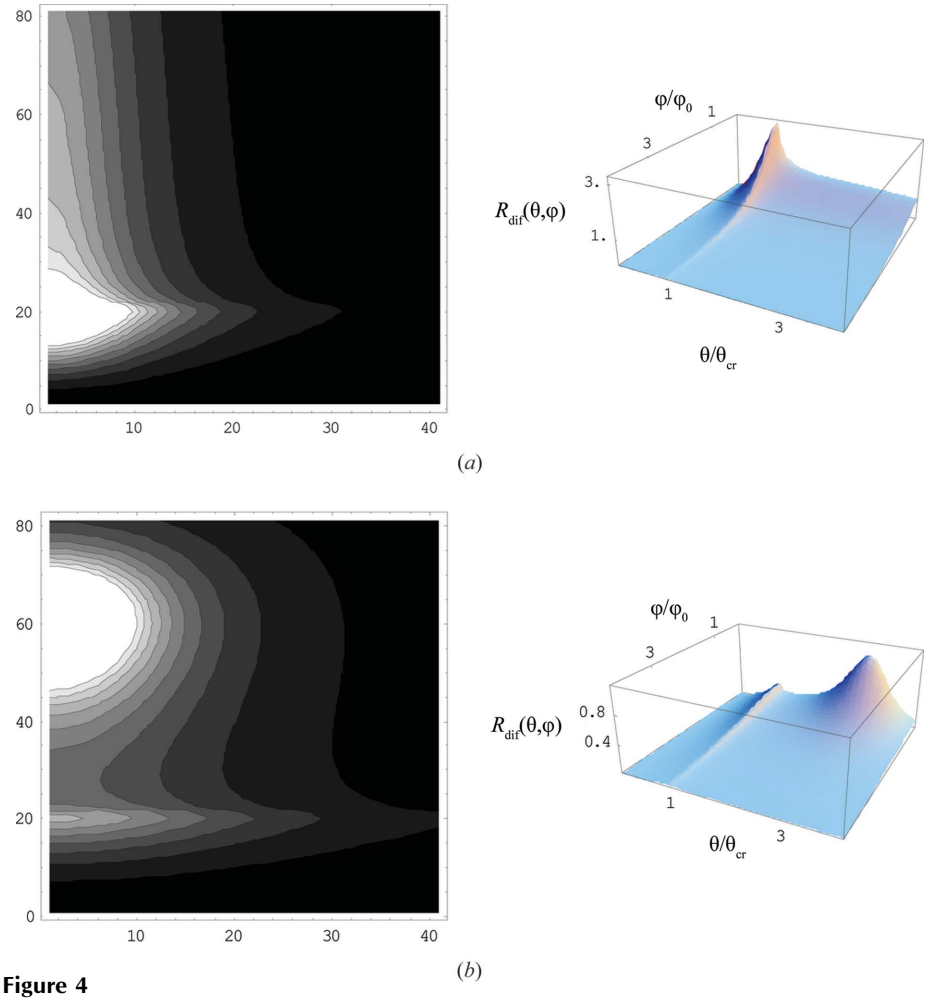

Figure 4
The numerically simulated two-dimensional contour plot and three-dimensional plot of the normalized GISAX $R_{\rm dif}(\theta,\varphi)/R_{\rm dif}(\theta_0,0)$ scans. The grazing incidence angle $\theta_0/\theta_{\rm cr}=3$. The dimensionless r.m.s. roughness $k\sigma=35$. The dimensionless cumulant correlation length $k\ell$: (*a*) $=5\times10^3$, (*b*) $=5\times10^4$.

Expression (28) is a manifestation of the fact that for $k\ell\theta_0 >> 1$ the integrated intensity of diffuse scattering $R_{\rm dif}^{\rm (int)}(\mathbf{q}_0)$ is mainly composed of the grazing scattering angle region $\Delta\theta\sim(k\ell\theta_0)^{-1}$ around $\theta=\theta_0$ and the azimuth angle region $\Delta\varphi\sim(k\ell)^{-1}$ close to $\varphi=0$ ($\varphi=0$ at specular).

Thus, mathematical foundations for describing the reflected GISAX scattering from random Gaussian surfaces condense into the formula assembly [equations (20)–(24)]. They are fundamentally based on implementing the self-consistent wavefunction approximation [equation (10)] to search the non-averaged solution of the integral wave equation (3) alongside the two-point cumulant correlation function approach for evaluating the statistical scattering factor [equation (21)]. Both these physical prerequisites seem to be very effective at providing the statistically averaged GISAX scattering intensity [equation (14)].

5. Numerical run-through for displaying the reflected GISAX diffuse scattering

Hereafter, the results of numerical calculations in the framework of the theoretical foundation proposed are presented and it is shown how the GISAX diffuse scattering from a random rough surface can be interpreted in terms of the surface parameters of interest.

As an example, using the theoretical expressions (21)–(24) and (29), the normalized statistical scattering factors $\eta(\theta,\theta_0)$ *versus* the grazing scattering angle $\theta/\theta_{\rm cr}$ are numerically evaluated for the two values of grazing incidence angle $\theta_0/\theta_{\rm cr}$: (Figs. 1*a* and 2*a*) = 2, (Figs. 1*b* and 2*b*) = 3 and the dimensionless r.m.s. roughness $k\sigma=35, 65$ (Figs. 1, 2). It is seen that both the numerically evaluated factors $\eta(\theta,\theta_0)$ as functions of $\theta/\theta_{\rm cr}$ have maxima close to the value of $\theta/\theta_{\rm cr}=1$. Respectively, in general, they provide peaks in the reflected GISAX diffuse scattering (Yoneda, 1963).

In the case when $\theta_0/\theta_{\rm cr}=2$ the calculated factors $\eta(\theta_0,\theta_0)$ are approximately two times more than the corresponding ones for $\theta_0/\theta_{\rm cr}=3$ for the same value of $k\sigma$ (*cf.* Figs. 1*a* and 2*a*, and Figs. 1*b* and 2*b*).

It is easy to see that the calculated factors $\eta(\theta_{\rm cr},\theta_0)$ at $\theta=\theta_{\rm cr}$ decrease (increase) with increasing (decreasing) r.m.s. roughness σ (see Figs. 1 and 2).

According to expression (27) the numerically simulated two-

dimensional contour plots and three-dimensional plots of the normalized GISAX diffuse scattering intensity $R_{dif}(\theta, \varphi)/R_{dif}(\theta, 0)$ are presented for the dimensionless r.m.s. roughness $k\sigma$: (Figs. 3 and 4) = 35, (Figs. 5 and 6) = 65. The following values have been assumed for the normalized grazing incidence angle θ_0/θ_{cr}: (Figs. 3, 5) = 2, (Figs. 4, 6) = 3 and dimensionless cumulant correlation length $k\ell$: (Figs. 3*a*, 4*a*, 5*a*, 6*a*) = 3.5×10^3, (Figs. 3*b*, 4*b*, 5*b*, 6*b*) = 4.5×10^4.

As follows from all the numerically simulated $R_{dif}(\theta, \varphi)/R_{dif}(\theta, 0)$ scans, they are a manifestation of the fact that when $\theta \simeq \theta_{cr}$, the GISAX diffuse scattering has a 'Yoneda scattering' peak (Yoneda, 1963), the magnitude of which depends strongly on the dimensionless cumulant correlation length $k\ell$: Yoneda's peak value rises (reduces) with decreasing (increasing) the dimensionless parameter $k\ell$.

Loosely speaking, any GISAX diffuse scattering intensity scan represents by itself the product of the two terms, the statistical scattering factor $\tilde{\eta}(\theta, \theta_0)$ and Fourier transform of the two-point cumulant correlation function. The statistical scattering factor $\tilde{\eta}(\theta, \theta_0)$ has a narrow maximum at $\theta \simeq \theta_{cr}$ (Yoneda's peak), whereas the Fourier transform of the two-point cumulant correlation function has a broader maximum at $\theta \simeq \theta_0$, the width of which depends on the dimensionless cumulant correlation length $k\ell$. That is a peculiarity of the normalized GISAX $R_{dif}(\theta, \varphi)/R_{dif}(\theta_0, 0)$ scan formation. One may clearly see it in Figs. 3–6, particularly as a shift of the second maximum of the $R_{dif}(\theta, \varphi)/R_{dif}(\theta_0, 0)$ scan as a function of incident angle θ in Fig. 3(*b*) where $\theta_0 = 2\theta_{cr}$ to Fig. 6(*b*), where $\theta_0 = 3\theta_{cr}$.

It needs to be remembered that, in averaging over random Gaussian surfaces, we have applied the two-point cumulant correlation function approach for splitting the X-ray scattering intensity into specular and diffuse scattering parts. It has allowed us to obtain the analytical expression [equations (19)–(20)] for both the specular and diffuse scattering waves. Once more, the case occurs where the two-point cumulant correlation function [equation (26)] is identical with the height–height correlation function, provided that the r.m.s. roughness σ is relatively small and the first-order Born approximation for solving the integral wave equation (3) works more or less well (*cf.* Vinogradov *et al.*, 1985).

At the same time, by evaluating the statistical scattering factor $\tilde{\eta}(q, q_0)$ in terms of the height–height correlation function [equation (16)] and comparing it with the corresponding expresssion given in terms of the two-point cumulant correlation function [equation (26)], one may link both the correlation functions.

As a result, based on the mathematical formalism elaborated and minimizing the GISAX diffuse scattering error functional, *e.g.* in the framework of a direct χ^2 fit algorithm iterative procedure in a least-square fashion, retrieving physical parameters of real rough surfaces from the experimental high-resolution diffuse scattering data becomes a reality.

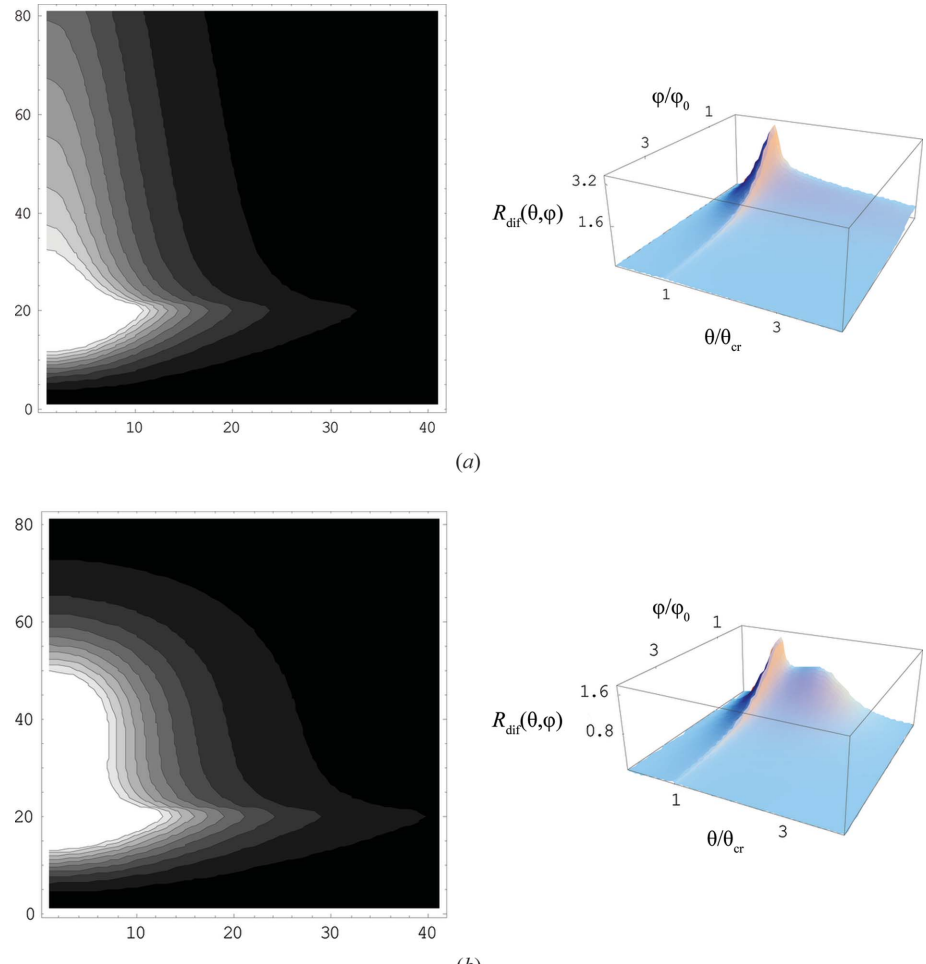

Figure 5
The numerically simulated two-dimensional contour plot and three-dimensional plot of the normalized GISAX $R_{dif}(\theta, \varphi)/R_{dif}(\theta_0, 0)$ scans. The grazing incidence angle $\theta_0/\theta_{cr} = 2$. The dimensionless r.m.s. roughness $k\sigma = 65$. The dimensionless cumulant correlation length $k\ell$: (*a*) = 5×10^3, (*b*) = 5×10^4.

6. Results and discussion

Analytical and numerical results presented in §§2–5 support the key idea of our study to go beyond the DWBA and the first-order Born approximation as well regarding the GISAX scattering. For this, the integral wave equation (3) provides a rigorous description of the X-ray wavefield propagation through the twofold medium and it is adjusted with the Green function formalism and the statistical model of a random Gaussian surface using the two-point cumulant correlation function approach. Unlike in the DWBA method, we have used the self-consistent approximation for

the wavefunction to find out the basic solution of the non-averaged equation (3). Such a solution has allowed us to describe the GISAX scattering for any scattering angles θ, in particular below the critical angle θ_{cr} for total external reflection. Expression (19) for the specular reflection obtained in terms of the self-consistent approximation agrees with the Fresnel expression multiplied by the Debye–Waller factor.

The analytical expressions for the statistical scattering factor $\tilde{\eta}(q, q_0)$ and reflected GISAX diffuse scattering $R_{dif}(\theta, \varphi)$ scan have been carried out for random Gaussian surfaces in terms of the r.m.s. roughness σ and cumulant correlation length ℓ.

The upper estimate of the GISAX diffuse scattering integral intensity [equation (28)] is presented at large values of $k\ell$ when the parameter $k\ell\theta_0$ is more than unity.

The run-through of the numerically simulated $R_{dif}(\theta, \varphi)$ scans for the typical parameter values of $\{\theta_0/\theta_{cr}, k\sigma, k\ell\}$ has been displayed. Basically, they have been the manifestation of the fact that their shape and contrast, in particular the appearance of Yoneda's peaks at $\theta \simeq \theta_{cr}$, mainly depend on the value of the parameter $k\ell$ associated with a random rough surface.

The present theoretical approach at its core is based on two major physical prerequisites.

One of them is that approximating the wavefunction near a random rough surface in a self-consistent sense is very important for searching the basic approach to solve the non-averaged integral wave equation. Another is that applying the rough-surface model in terms of the two-point cumulant correlation function seems to be effective for providing a statistical average of the reflected GISAX intensity concerning specular and diffuse scattering. Both these physical assumptions have allowed us to model the $R_{dif}(\theta, \varphi)$ scans regarding the GISAX scattering from random rough surfaces.

On the other hand, the latter can be applied for analysing the experimental GISAX diffuse scattering from random rough surfaces (*e.g.* in the framework of an iterative χ^2 fit procedure) and, finally, to retrieve physical information concerning the roughness characteristics and the length scales of the order of the height–height correlation length.

It should be mentioned once more that the theoretical approach presented is valid only for a random Gaussian surface that models real solid surfaces quite well, as pointed out in Sinha *et al.* (1988).

The question of whether this theoretical approach has any validity in cases of real solid surfaces [*e.g.* if the roughness is highly correlated with the atomic arrangements; see Sinha *et al.* (1988) for more detailed discussion] or whether it should be given up in favour of other approaches, which should be developed anew, remains a good topic for future work.

To be specific, of greater interest may be future investigation to justify the present theoretical approach for evaluating the reflected GISAX diffuse scattering by implementation of a general cumulant average technique (Polyakov *et al.*, 1991).

Finally, it is hoped that modelling the reflected GISAX diffuse scattering angular scans in terms of the presented self-consistent wavefunction approximation and statistical approach based on the two-point cumulant correlation function can be favourably applied to the retrieval of physical parameters of real solid and liquid surfaces using experimental high-resolution X-ray scattering data.

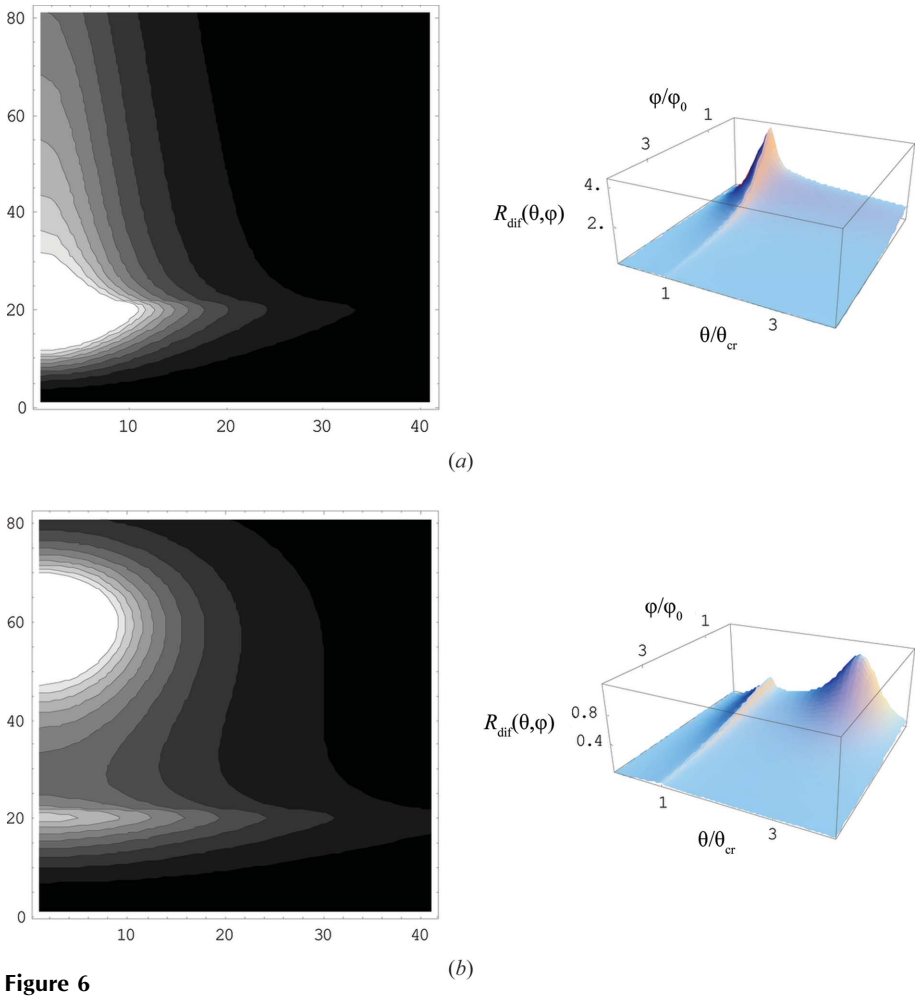

Figure 6
The numerically simulated two-dimensional contour plot and three-dimensional plot of the normalized GISAX $R_{dif}(\theta, \varphi)/R_{dif}(\theta_0, 0)$ scans. The grazing incidence angle $\theta_0/\theta_{cr} = 3$. The dimensionless r.m.s. roughness $k\sigma = 65$. The dimensionless cumulant correlation length $k\ell$: (*a*) = 5×10^3, (*b*) = 5×10^4.

Valuable discussions with V. A. Bushuev, I. V. Kozhevnikov, A. M. Polyakov and S. V. Salikhov are gratefully acknowledged.

References

Boer, D. K. G. de (1994). *Phys. Rev. B Condens. Matter*, **49**, 5817–5823.

Boer, D. K. G. de (1995). *Phys. Rev.* **51**, 5297–5302.

Bridou, F., Gauthier, J., Delmore, F., Ravet, M.-F., Durand, O. & Modreanu, M. (2006). *Appl. Surf. Sci.* **253**, 12–16.

Chukhovskii, F. N. (2009). *Acta Cryst.* A**65**, 39–45.

Chukhovskii, F. N. & Polyakov, A. M. (2010). *Acta Cryst.* A**66**, 640–648.

Gilles, R., Lazzari, R. & Leroy, F. (2009). *Surf. Sci. Rep.* **64**, 255–380.

Kato, N. (1980). *Acta Cryst.* A**36**, 763–769.

Lazzari, R. (2002). *J. Appl. Cryst.* **35**, 406–421.

Levine, J. R., Cohen, J. B., Chung, Y. W. & Georgopoulos, P. (1989). *J. Appl. Cryst.* **22**, 528–532.

Mandelbrodt, B. B. (1982). *The Fractal Geometry of Nature*. New York: Freeman.

Nevot, L. & Croce, P. (1980). *Rev. Phys. Appl.* **15**, 761–779.

Petrashen', P. V., Kov'ev, E. K., Chukhovskii, F. N. & Degtyarev, Yu. L. (1983). *Solid State Phys.* **25**, 1211–1214.

Pietsch, U., Holy, V. & Baumbach, T. (2004). *High-Resolution X-ray Scattering – From Thin Films to Lateral Nanostructures.* Berlin: Springer Verlag.

Polyakov, A. M., Chukhovskii, F. N. & Piskunov, D. I. (1991). *Sov. Phys. JETF*, **72**, 330–340.

Schmidbauer, M., Schäfer, P., Besedin, S., Grigoriev, D., Köhler, R. & Hanke, M. (2008). *J. Synchrotron Rad.* **15**, 549–557.

Sinha, S. K., Sirota, E. B., Garoff, S. & Stanley, H. B. (1988). *Phys. Rev. B*, **38**, 2297–2311.

Vinogradov, A. V., Zorev, N. N., Kozhevnikov, I. V. & Yakushkin, I. G. (1985). *Sov. Phys. JETF*, **62**, 1225–1233.

Voss, R. F. (1985). In *Scaling Phenomena in Distorted Systems*, edited by R. Pynn & A. Skjeltorp. New York: Plenum.

Yoneda, Y. (1963). *Phys. Rev.* **131**, 2010–2013.

Zozulya, A. V., Yefanov, O. M., Vartanyants, I. A., Mundboth, K., Mocuta, C., Metzger, T. H., Stangl, J., Bauer, G., Boeck, T. & Schmidbauer, M. (2008). *Phys. Rev. B*, **78**, 121304.